

Evidence for $B \rightarrow K^* \ell^+ \ell^-$ and Measurement of $B \rightarrow K \ell^+ \ell^-$

Anders Ryd on behalf of the BABAR collaboration^a

California Institute of Technology, Pasadena CA 91125

Received: xxyyzz / Revised version: xxyyzz

Abstract. We present evidence for the flavor-changing neutral current decay $B \rightarrow K^* \ell^+ \ell^-$ and a measurement of the $B \rightarrow K \ell^+ \ell^-$ branching fraction, where $\ell^+ \ell^-$ is either an $e^+ e^-$ or $\mu^+ \mu^-$ pair. The data sample analyzed comprises 88.5×10^6 $\Upsilon(4S) \rightarrow B \bar{B}$ decays collected with the BABAR detector at the PEP-II $e^+ e^-$ storage ring. Averaging over $K^{(*)}$ isospin and lepton flavor, we obtain $\mathcal{B}(B \rightarrow K^* \ell^+ \ell^-) = (1.40_{-0.49}^{+0.57} \pm 0.21) \times 10^{-6}$ and $\mathcal{B}(B \rightarrow K \ell^+ \ell^-) = (0.68_{-0.15}^{+0.17} \pm 0.04) \times 10^{-6}$, where the uncertainties are statistical and systematic. The significance for the $B \rightarrow K^* \ell^+ \ell^-$ signal is 3.0σ and for $B \rightarrow K \ell^+ \ell^-$ the signal significance is over 7σ .

PACS. 13.25.Hw – 13.20.He

1 Introduction

The decays $B \rightarrow K \ell^+ \ell^-$ and $B \rightarrow K^* \ell^+ \ell^-$ are examples of flavor-changing neutral current decays that at the quark level are mediated with a $b \rightarrow s$ transition. In the standard model (SM) there are no tree level $b \rightarrow s$ transitions. However, at one-loop order these decays proceed via diagrams containing a top quark and a W , as shown in Fig. 1. Because these decays only take place at higher order in the SM these decays are highly suppressed and new physics, *e.g.*, supersymmetric particles, can contribute at the same order as the SM contributions. This makes these decays an interesting place to look for new physics [1]. In the SM the predictions [1,2] for the $B \rightarrow K \ell^+ \ell^-$ branching fraction is in the range $(3 \text{ to } 6) \times 10^{-7}$ and the $B \rightarrow K^* \ell^+ \ell^-$ branching fraction is in the range $(1 \text{ to } 2) \times 10^{-6}$. The uncertainty on these predictions are dominated by the form factor uncertainties for the production of the K and K^* final states. The theoretical uncertainties on the inclusive branching fraction $B \rightarrow X_s \ell^+ \ell^-$ is smaller [1], about 10%.

This talk describes an analysis of the BABAR data sample of 81 fb^{-1} , corresponding to 88.5×10^6 $B \bar{B}$ pairs, collected at the $\Upsilon(4S)$ resonance. In this analysis we have used both electrons and muons in the final states, and for the hadronic system in the final state we have used K_S^0 , K^+ , $K^{*0} \rightarrow K^+ \pi^-$, and $K^{*+} \rightarrow K_S^0 \pi^+$ with $K_S^0 \rightarrow \pi^+ \pi^-$. Charge conjugate modes are implied everywhere.

We fully reconstruct the B candidates and apply strict particle identification criteria to all particles. The signal is identified using two kinematic variables,

$$m_{\text{ES}} = \sqrt{E_{\text{beam}}^2 - p_B^2},$$

^a Present address: Cornell University, Ithaca NY 14853

the energy substituted mass, that will peak at the B mass for signal candidates and ΔE , the energy difference between the reconstructed B energy and the known B energy from the beam energy. ΔE will peak at zero for signal candidates. The signal yield is extracted using an unbinned maximum likelihood fit in the m_{ES} and ΔE plane. In the K^* modes we in addition use the $m_{K\pi}$ mass distribution in the likelihood fit.

2 Event selection

In this analysis we make use of the charged particle tracking and particle identification capabilities of the BABAR detector. The BABAR detector is described in detail in Ref. [3]. We select events that contain at least four charged tracks. Two of these tracks are required to be identified as a pair of oppositely charged leptons. We require electron and muon candidates to have a momentum greater than 0.5 GeV and 1.0 GeV, respectively. Charged kaon candidates are required to be positively identified, primarily using information from the detector of internally reflected

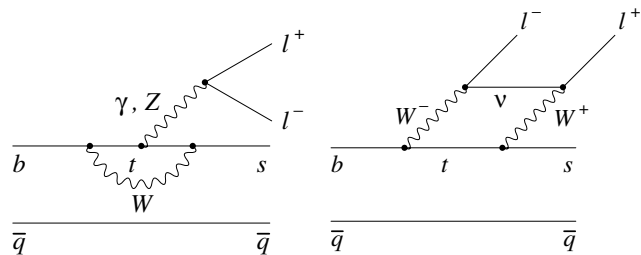


Fig. 1. Quark-level diagrams that contribute to $B \rightarrow K^{(*)} \ell^+ \ell^-$ in the SM.

Cherenkov radiation. The pion candidates in K^* candidates are required not to pass the kaon selection criteria. K_S candidates are reconstructed from two oppositely charged tracks that form a good vertex. The K_S vertex is required to be separated by at least 1 mm from the interaction point and have a momentum vector that is pointing back to the interaction point.

2.1 Backgrounds

As the branching fractions we are aiming to measure are very small we have to be very careful about backgrounds. We classify the backgrounds in the following way

- Combinatorial backgrounds that don't peak in the signal region.
 - From continuum production of u , d , s , and c quark-anti-quark pairs in the e^+e^- annihilation.
 - Combinatorics from $B\bar{B}$ events, where tracks from both B mesons are used.
- Backgrounds that peak in the signal region. This background comes from events where all candidates are coming from one B meson.
 - $B \rightarrow J/\psi K^{(*)}$ and $B \rightarrow \psi(2S) K^{(*)}$ decays where the J/ψ or $\psi(2S)$ decays to a pair of leptons.
 - Hadronic B meson decays where two of the hadrons are misidentified as leptons. This is a non-negligible background in the muon modes where the probability that a hadron is identified as a muon is higher than for an electron.

The combinatorial backgrounds in continuum events are suppressed using a Fisher discriminant [4] that provides separation between the signal and the continuum background. The Fisher discriminant is a linear combination of variables such as the events shapes [5], the reconstructed B production angle in the center-of-mass frame, and the invariant mass of the $K\ell$ system.

To suppress the combinatorial background in $B\bar{B}$ events we form a likelihood to separate the signal from the background. The likelihood includes the missing energy in the event and vertex probabilities. The missing energy is the most powerful variable as the background in $B\bar{B}$ events is largely due to the real leptons from semileptonic decays that have a large missing energy due to the undetected neutrinos.

Peaking backgrounds are suppressed using specialized vetoes. The most serious background is from the charmonium decays of the B . We apply a cut on the dilepton mass, $m_{\ell\ell}$, to veto events that have a dilepton mass consistent with the either the J/ψ or $\psi(2S)$. In addition we veto, in the muon modes, certain hadronic decays such as $B^- \rightarrow D^0 \pi^-$, with $D^0 \rightarrow K^- \pi^+$ by requiring that the kaon candidate and the oppositely charge lepton candidate has a mass that is not consistent with a D^0 .

In the electron channels we also veto electron candidates that are consistent with coming from photon conversions. In the $B \rightarrow K e^+ e^-$ modes we reject any electron that forms a good vertex with another track that has an invariant mass less than 50 MeV. In the $B \rightarrow K^* e^+ e^-$

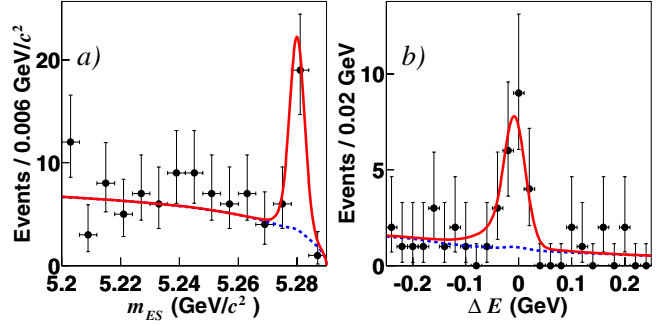


Fig. 2. Projections of the likelihood fit on m_{ES} and ΔE in the combined $B \rightarrow K \ell^+ \ell^-$ fit.

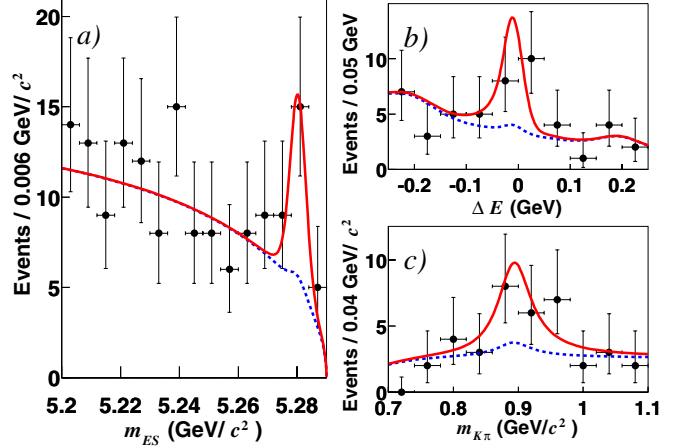


Fig. 3. Projections of the likelihood fit on m_{ES} and ΔE and $m_{K\pi}$ in the combined $B \rightarrow K^* \ell^+ \ell^-$ fit.

modes we require that the vertex is separated from the interaction point by 1.5 cm. To preserve efficiency at low q^2 where we have a pole in the K^* modes we do not require the vertex separation.

With these selection criteria we find an average of 0.12 ± 0.05 events in the $B \rightarrow K^* \ell^+ \ell^-$ modes and an almost negligible peaking background in the $B \rightarrow K \ell^+ \ell^-$ modes.

3 Results

To extract the signal yield we perform an unbinned maximum likelihood fit in the m_{ES} - ΔE plane. In the modes containing a K^* we also include the $K\pi$ mass in the fit. The fit contains several different components. The signal shape is determined from signal Monte Carlo samples, though the mean m_{ES} and ΔE are taken from fits to the charmonium control samples in the data. The combinatorial background component is modeled as an ARGUS function [6] in m_{ES} and an exponential in ΔE . We also include a component for the peaking background where the yield is fixed from Monte Carlo simulation and control samples in the data. The results of the fits are summarized in Table 1. The top portion of the table contains

Table 1. Results from the fits to $B \rightarrow K^{(*)} \ell^+ \ell^-$ modes. The columns are, from left to right: fitted signal yield; the signal efficiency, ϵ (not including the branching fractions for K^* and K^0 decays); the systematic error on the selection efficiency, $\Delta\mathcal{B}_\epsilon/\mathcal{B}_\epsilon$; the systematic error from the fit, $\Delta\mathcal{B}_{\text{fit}}$; and the branching fraction central value (\mathcal{B}). For the combined channels, the signal yields are efficiency-corrected.

Mode	Signal yield	ϵ (%)	$\Delta\mathcal{B}_\epsilon/\mathcal{B}_\epsilon$ (%)	$\Delta\mathcal{B}_{\text{fit}}$ (10^{-6})	\mathcal{B} (10^{-6})
$K^+ e^+ e^-$	$16.2^{+4.8}_{-4.1}$	19.1	± 5.6	± 0.04	$0.96^{+0.28}_{-0.24} \pm 0.07$
$K^+ \mu^+ \mu^-$	$1.0^{+2.0}_{-1.2}$	8.7	± 6.8	± 0.01	$0.14^{+0.25}_{-0.16} \pm 0.02$
$K^0 e^+ e^-$	$-0.5^{+1.2}_{-1.0}$	20.6	± 11.9	± 0.02	$-0.08^{+0.25}_{-0.16} \pm 0.02$
$K^0 \mu^+ \mu^-$	$5.0^{+2.8}_{-2.0}$	9.2	± 12.4	± 0.01	$1.78^{+0.99}_{-0.73} \pm 0.22$
$K^{*0} e^+ e^-$	$7.8^{+5.4}_{-4.2}$	13.5	± 6.7	± 0.12	$0.98^{+0.68}_{-0.54} \pm 0.14$
$K^{*0} \mu^+ \mu^-$	$4.5^{+3.8}_{-2.8}$	6.5	± 13.6	± 0.04	$1.18^{+0.99}_{-0.73} \pm 0.12$
$K^{*+} e^+ e^-$	$2.7^{+4.1}_{-2.9}$	10.2	± 15.3	± 0.01	$1.31^{+1.97}_{-1.38} \pm 0.18$
$K^{*+} \mu^+ \mu^-$	$4.4^{+3.5}_{-2.4}$	5.0	± 10.6	± 0.01	$4.33^{+3.41}_{-2.40} \pm 0.66$
Ke^+e^-	63^{+19}_{-16}		± 5.8	± 0.02	$0.71^{+0.21}_{-0.18} \pm 0.05$
$K\mu^+\mu^-$	52^{+28}_{-22}		± 6.9	± 0.02	$0.59^{+0.32}_{-0.25} \pm 0.04$
$K\ell^+\ell^-$	60^{+15}_{-13}		± 5.8	± 0.01	$0.68^{+0.17}_{-0.15} \pm 0.04$
$K^*e^+e^-$	90^{+56}_{-46}		± 6.8	± 0.11	$1.02^{+0.63}_{-0.52} \pm 0.13$
$K^*\mu^+\mu^-$	156^{+88}_{-70}		± 9.8	± 0.23	$1.77^{+0.95}_{-0.79} \pm 0.29$
$K^*\ell^+\ell^-$	124^{+50}_{-44}		± 7.0	± 0.19	$1.40^{+0.57}_{-0.49} \pm 0.21$

the results of the fits in the eight individual modes. The lower part of the table contains the results of combined fits where we have averaged over lepton flavor and isospin. For the $B \rightarrow K^* \ell^+ \ell^-$ average we have used the constraint $\mathcal{B}(B \rightarrow K^* e^+ e^-) = 1.33 \times \mathcal{B}(B \rightarrow K^* \mu^+ \mu^-)$ by Ali *et al.* in Ref. [1]. The combined branching fraction is quoted as a branching fraction for the $B \rightarrow K^* e^+ e^-$ process. The projection of these fits are shown in Figs. 2 and 3

Systematic uncertainties have been evaluated for the effects of detector efficiency simulation, model dependence, and background estimation. The signal significances for the combined $B \rightarrow K^* \ell^+ \ell^-$ and $B \rightarrow K \ell^+ \ell^-$ modes have been evaluated to be 3.0σ and over 7σ respectively.

4 Summary

In summary we have measured the branching fraction for $B \rightarrow K \ell^+ \ell^-$ with a significance of over 7σ and obtained the first evidence for the decay $B \rightarrow K^* \ell^+ \ell^-$ with a significance of 3.0σ . We find the following branching fractions

$$\mathcal{B}(B \rightarrow K \ell^+ \ell^-) = (0.68^{+0.17}_{-0.15} \pm 0.04) \times 10^{-6}, \quad (1)$$

$$\mathcal{B}(B \rightarrow K^* \ell^+ \ell^-) = (1.40^{+0.57}_{-0.49} \pm 0.21) \times 10^{-6} \quad (2)$$

where the $B \rightarrow K^* \ell^+ \ell^-$ branching fraction is quoted as a branching fraction for $B \rightarrow K^* e^+ e^-$. These branching fractions are in agreement with the standard model predictions.

Since the presentation of this result we have updated the analysis to include a sample of 113 fb^{-1} , corresponding to $(122.9 \pm 1.4) \times 10^6 B\bar{B}$ pairs [7]. The results obtained [7],

$$\mathcal{B}(B \rightarrow K \ell^+ \ell^-) = (0.65^{+0.14}_{-0.13} \pm 0.04) \times 10^{-6}, \quad (3)$$

$$\mathcal{B}(B \rightarrow K^* \ell^+ \ell^-) = (1.17^{+0.44}_{-0.26} \pm 0.13) \times 10^{-6} \quad (4)$$

are consistent with the results presented here. The significance of the $B \rightarrow K^* \ell^+ \ell^-$ signal is 3.3σ , including systematic uncertainties.

References

1. A. Ali *et al.*, Phys. Rev. D **66**, 034002 (2002); G. Burdman, Phys. Rev. D **52**, 6400 (1995); J.L. Hewett and J.D. Wells, Phys. Rev. D **55**, 5549 (1997).
2. A. Ali *et al.*, Phys. Rev. D **61**, 074024 (2000); P. Colangelo *et al.*, Phys. Rev. D **53**, 3672 (1996); D. Melikhov, N. Nikitin, and S. Simula, Phys. Rev. D **57**, 6814 (1998); T.M. Aliev *et al.*, Phys. Lett. B **400**, 194 (1997); T.M. Aliev, M. Savci, and A. Özpıneci, Phys. Rev. D **56**, 4260 (1997); C.-H. Chen and C.Q. Geng, Phys. Rev. D **66**, 094018 (2002); H.-M. Choi, C.-R. Ji, and S. Kisslinger, Phys. Rev. D **65**, 074032 (2002); N.G. Deshpande and J. Trampetic, Phys. Rev. Lett. **60**, 2583 (1988); A. Faessler *et al.*, Eur. Phys. J. direct C **4**, 18 (2002); C. Greub, A. Ioannissian, and D. Wyler, Phys. Lett. B **346**, 149 (1995); C.Q. Geng and C.P. Kao, Phys. Rev. D **54**, 5636 (1996); M. Zhong, Y.L. Wu, and W.Y. Wang, Int. J. Mod. Phys. A **18**, 1959 (2003).
3. BABAR Collaboration, B. Aubert *et al.*, Nucl. Instrum. Methods A **479**, 1 (2001).
4. R.A. Fisher, Ann. Eugenics **7**, 179 (1936).
5. G.C. Fox and S. Wolfram, Phys. Rev. Lett. **41**, 1581 (1978).
6. The function is $f(x) \propto x\sqrt{1-x^2} \exp[-\zeta(1-x^2)]$, where ζ is a fit parameter and $x = m_{\text{ES}}/E_b^*$; ARGUS Collaboration, H. Albrecht *et al.*, Z. Phys. C **48**, 542 (1990).
7. BABAR Collaboration, B. Aubert *et al.*, Phys. Rev. Lett. **91**, 221802 (2003). The combined $B \rightarrow K^* \ell^+ \ell^-$ branching fraction is given for the muon modes. To compare with the result presented in this talk I have converted the branching fraction to the electron final state.